Tuijin Jishu/Journal of Propulsion Technology
ISSN: 1001-4055
Vol. 45 No. 3 (2024)

Structural and Electrical Properties of Ultrafine $Li_{0.43}Zn_{0.195}Fe_{2.37}O_4$ Ferrite Powder Synthesized by a Freeze-Drying Process

Mohammed Al-Baidhani [1], Noorhan S. Jumaah [2], Mays A. Wahish [3], Saad Oboudi [4]*

[1, 2, 3] *Department Physics, College of Science, Al Nahrain University*

[4] *Center of Advanced Materials Research, University of Sharjah, Sharjah, United Arab Emirates*

Abstract:- Zinc-substituted lithium (LiZn) ferrite with the general formula $Li_{0.43}Zn_{0.195}Fe_{2.37}O_4$ was prepared by using the freeze-drying method. The phase purity, homogeneity, lattice structure, and cell parameters of the prepared samples were carried out using the XRD technique which indicates the formation of a single-phase cubic structure. The dielectric constant (**ε'**) was measured as a function of frequency and temperature by using the two-probe technique. It is found that the dielectric constant decrease continuously with the increase of frequency without any change in the Curie temperature. The electrical conductivity (Lnσ) shows a decrease with increase in frequency for all the samples. The reduction in the dielectric constant at higher frequencies has been explained by the fact that beyond a certain frequency, the electronic exchange between ferrous and ferric ions cannot follow the frequency of the alternating field.

Keywords*: Lithium ferrite, Freeze drying, Dielectric behavior.*

1. Introduction

Lithium ferrites have attracted the attention of scientists for their interesting features and their low cost, which makes them substitute for expensive magnetic garnets. They are generally having vast applications from microwave to radio frequency regions [1,2]. The low electrical conductivity makes this type of ferrite attractive material, especially for microwave applications. The order of magnitude of the conductivity greatly influences the electric and magnetic behavior of ferrites where the spinel lithium ferrite contains Fe^{+2} and lithium ions and therefore it is expected that this material exhibits both electronic and ionic conductivities [3]. The modifications of the different properties of ferrites due to the substitution of divalent, trivalent, and tetravalent ions have been studied by several authors [4,5]. The substituted lithium ferrites are advantageous due to their application potential in the microwave frequency range.

Lithium–zinc ferrite is a pertinent magnetic material for applications because of its better properties at high frequency and lower densification temperatures than other ferrites. It is prominent that the intrinsic parameters of high-frequency lithium–zinc depend on the composition, technological factors, and additives or substitutions as well as the other preparation conditions. The reduction of porosity is a problem in Li–Zn ferrite because the lithium volatility and oxygen loss imply a limitation on the sintering temperature. By introducing a relatively small amount of foreign ions an important modification of both structure and magnetic properties can be obtained [6,7]. By introducing nonmagnetic ions such as Zn^{+2} in Li–ferrite a very large influence on several of its magnetic properties such as magnetization, magnetic susceptibility, Curie temperature, etc. takes place. Zn^{+2} ions also have a considerable effect on other properties of lithium ferrite like B site ordering, dielectric behavior, electrical resistivity, etc. [8].

Surzhikov et al. [9] showed that the use of high-energy electron beam heating allows obtaining high-quality LiZn ferrite ceramics at (1050–1100) °C temperature range for 2 h.and Malyshev et al. [10] studied the use of two types of high-energy electron beam heating (pulsed or continuous) extending the possibility to use radiation-thermal

technology for LiZn ferrites production. Liu et al. [11] investigated the addition of Bi_2O_3 and showed that it greatly improved the sintered density and promoted the grain growth of LiZn ferrites as a reaction center at a lower temperature. However, the partial agglomeration of Bi_2O_3 on the grain boundary restrained abnormal grain growth at higher sintering temperatures. The effect of the replacement of divalent Zn^{+2} ions on the electrical, magnetic, structural properties, and thermoelectric power of Li ferrite samples was investigated in this paper.

2. Experimental

The Zn-substituted lithium ferrite samples having the general formula $Li_{0.43}Zn_{0.195}Fe_{2.37}O_4$ were prepared by using the freeze-drying method. A stoichiometric mixture was prepared from the raw materials Li $C_2H_3O_2.2H_2O$ Lithium acetate, Fe $C_6H_6O_7.5H_2O$ Ferrite citrate, and Zn $(C_2H_3O_2)_2.2H_2O$ Zinc acetate. These powders were preferred to the nitrates because of their lower temperature of decomposition below 200ºC which will not result in loss of the fine particle nature by an increase of grain size during the heat treatment. Since the role of chemical purity has been found to be extremely significant, a purity level of 99.9% and distilled water were used. The sample preparation process takes place through the following stages: The raw materials were dissolved in (200 ml) of distilled water. The mixed solution was heated at a temperature of about (80 ºC), with continuous stirring, then sprayed as an aerosol into a dish containing liquid nitrogen, which produced rapid freezing of droplets. The sprayed droplets, ranging in size from (100 to 300 μm), were then dried by sublimation (lyophilization), under a cooling temperature of about (-33ºC) and primary vacuum pressure in the range of (3.3×10^{-3} mbar). The resultant powders were heated at (150ºC) for (30 min) in order to remove the acetates and citrates as gaseous from the mixture leaving behind a desired product as oxides fine powder.

Finally, the powders were pressed into pellets (1.2 cm) in diameter. The sintering of the samples was carried out at 750ºC for 2 hrs and the final sintering at 1000ºC for 5 hrs in air. X-ray diffraction was performed using an X-ray diffractometer with Cu Ka (λ =1.5418 Å) radiation. The single-phase formation was confirmed by X-ray diffraction patterns. The real part of the dielectric constant (ε') and ac electrical conductivity (lnσ) were measured using a Hioki LCR meter at different temperatures (300–800 K) as a function of frequency (1 KHz–500KHz). The values of ε' were calculated from the capacitance (c) using the formula :

$$\varepsilon' = cd / \varepsilon_o A \quad (1)$$

where d is the thickness of the sample, A is the cross-sectional area of the flat surface of the pellet and ε_o is the free-space permittivity. The temperature of the samples was measured using a K-type thermocouple with a junction in contact with the sample to obtain the exact temperature.

3. Results and Discussion

A. X-rays diffraction

From the X-rays diffraction pattern, it is clear that the synthesized Zn-substituted lithium ferrite compounds are single-phase and that all samples crystallize in the same group. Fig. 1 shows the refinement. Furthermore, it was found that all the samples crystallize corresponding to the face center cubic (fcc) structure with the Pm3m space group. No diffraction peaks of other impurities were observed, which indicates the high purity of the final products. The values of lattice parameter 'a' were calculated for different samples and were found to be (a=8.34453, b=8.34453, and c=8.34453).

B. SEM micrograph

Fig. 2 shows the microstructure of the prepared samples. The SEM micrograph of the freeze-dried powders seems to be agglomerated in aggregates. The shape is caused by material displacement induced by ice crystals' growth during freezing. Contrary to expectation, the lower initially-concentrated powder shows a denser microstructure with an average grain size of about 5 μm. This can be explained by the greater brittleness of such a structure built upon a more fine agglomerate. So, the slightest handling makes it collapse [12,13].

C. The dielectric constant ε′

Fig. 3 is a typical curve showing the relation between the real part of the dielectric constant ε′ and absolute temperature (T) from 380K to 580K as a function of the applied frequency ranging from 1 KHz to 500KHz. It can be seen from the figure that the value of ε′ decreases continuously with increasing frequency without any change in the Curie temperature (Tc). This decrease of ε′ with increasing frequency is a general trend that is due to the scattering of charge carriers as they cannot follow the fast variation of the electric field accompanied by the applied frequency. In addition, this reduction occurs because beyond a certain frequency of the externally applied electric field, the electronic exchange between ferrous and ferric ions, i.e. $Fe^{+2} \rightarrow Fe^{+3} + e^{-}$ is fast and the formed dipoles cannot follow the field variations. This behavior of ε′ is explained qualitatively by the assumption that the mechanism of polarization and conduction processes are of the same origin. A similar temperature variation of the dielectric constant has been reported earlier [13–15].

D. The electrical conductivity lnσ

The variation of of lnσ (S cm^{-1}), where S =Ω^{-1} (Simons) versus temperature 1000 T^{-1} (K^{-1}) for the samples is represented in Fig. 4. Throughout the whole temperature range [300–700 K], the material exhibits a semiconductor behavior. There was no metal-insulator transition. The behavior is similar to that of similar ferrites with a change in the slopes of the straight lines at a certain temperature, which corresponds to the Curie temperature indicating the different conduction mechanisms.

E. The activation energy ΔE

The activation energy of the different regions was calculated from the experimental data using the relation:

$$\sigma = \sigma_o \exp(-\Delta E/kT) \quad (2)$$

where ΔE represents the activation energy, σ is the conductivity at temperature T, so is a temperature-independent constant, and k is the Boltzmann constant. It is clear from the figure that the value of lnσ increases almost linearly with increasing temperature up to a certain temperature at which the slopes of lines are varied. This means that the ferrimagnetic material transforms to paramagnetic at the Curie temperature. This indicates that the Li–Zn ferrite samples in this study exhibit semiconducting behavior and the values of the activation energy for electric conduction Ei in the ferrimagnetic and Eii in the paramagnetic regions enhance this behavior. The activation energy values are tabled in Table 1.

It is interesting to note that the value of the Curie temperature (Tc) is found to decrease continuously with increasing frequency. This means that the weakening of the AB interaction increases with zinc content which causes a decrease in the Curie temperature as mentioned by other authors in mixed Ni–Zn ferrites and Li–Zn ferrites [16–18].

Accordingly, the conduction at lower temperature region (below Curie temperature) is due to the hopping of electrons between Fe^{+2} and Fe^{+3} ions and holes due to the replacement of a small ionic radius (r_{Li} = 0.60Å) of monovalent Li^{+1} ions on the expense of relatively larger Fe^{+3} (r_{Fe} 0:64 Å) on octahedral (B) site. While; at higher temperatures (above Curie temperature) it is due to polaron hopping in addition to the electron hopping between iron ions of different valances which is the most predominant one in this region [19]. The presence of Fe^{+3} and Fe^{+2} simultaneously on the B-sites plays a significant role in the conduction process according to the electron exchange between these two ions. While the presence of Zn^{+2} and Li^{+1} ions on A-sites makes bears p-type conduction. This means that the two conduction processes are present and the sample is partly compensated due to the simultaneous presence of acceptor and donor centers [20]. The polarization in the tetrahedral sites is opposite to that of octahedral sites, which depends on the cation distribution on both sites.

4. Conclusions

Zn substituted lithium ferrite powders, with average particle sizes of 5 μm were prepared by a freeze-drying method. These powders have good sinter ability, and samples with no liquid-phase agents can be sintered at (1000 ^{o}C). All the samples with the Zn lithium ferrite phase were with typical spinel structures. The dependence of the

dielectric constant on the applied frequency for the investigated samples shows that the decrease of ε′ with increasing frequency is a general trend.

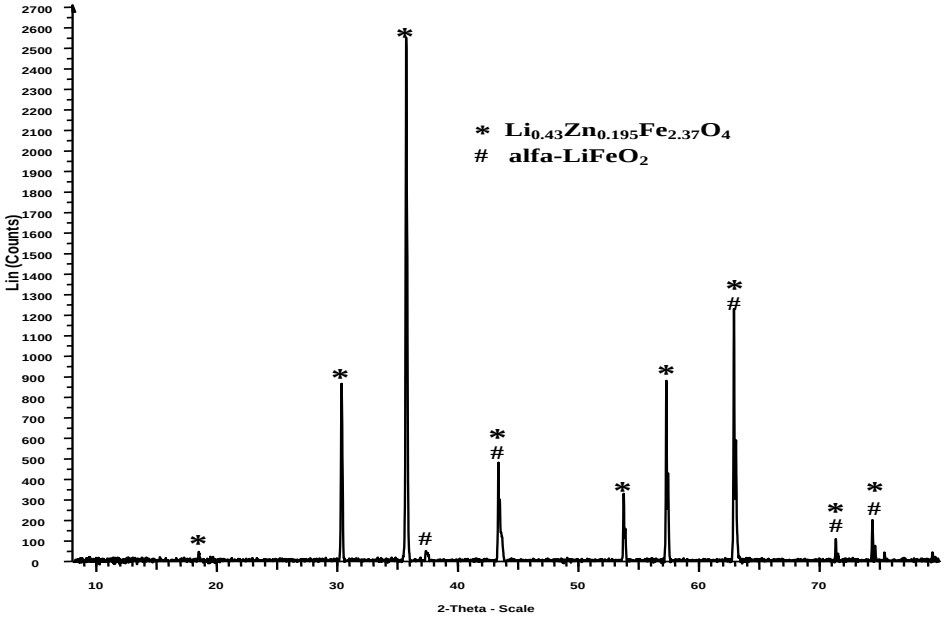

Fig. 1 $Li_{0.43}Zn_{0.195}Fe_{2.37}O_4$ Cubic - a 8.34453 - b 8.34453 - c 8.34453 alpha 90.000 - beta 90.000 - gamma 90.000 - Face-center

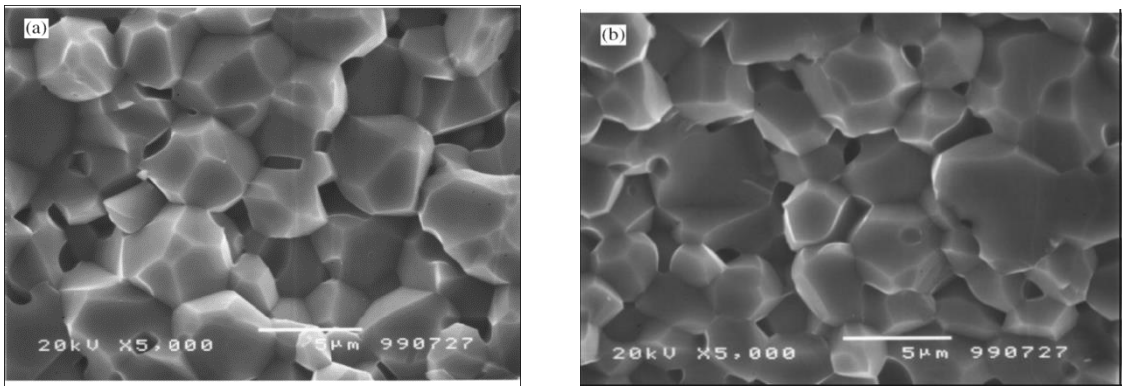

Fig. 2 SEM images of the fracture surface

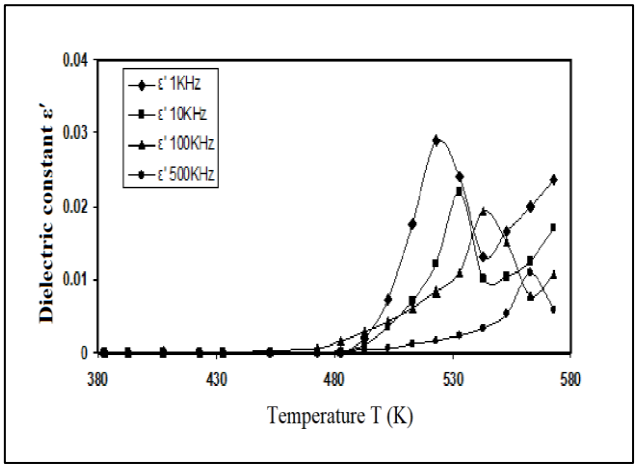

Fig. 3 Dependence of ε′ on the absolute Temperature T (K) as a function of frequency

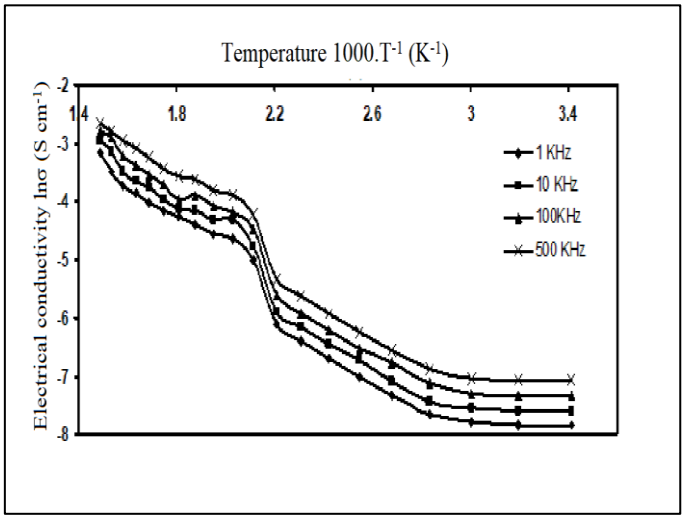

Fig. 4 The relation between the electrical conductivity (ln σ) and Temperature 1000.T^{-1} (K^{-1})

Table 1. Activation energy values Ei and Eii at different values of frequency.

Frequency	Ea i	Ea ii
1 kHz	0.**000558**	**0.000429**
10 kHz	**0.000613**	**0.000423**
100 kHz	**0.00062**	**0.00041**
500 kHz	**0.000488**	**0.000429**

References

[1] S. S. Suryavanshi, S. M. Kabbur, U.B. Deshmukh, Sawant S.R, Journal of Electronic Materials, vol. 29, No.7, pp. 979-983, 2000.
[2] B. K. Kumar, G.P. Srivastava, Proc. Int. Conf. Ferrites, India vol. 5, pp. 227, 1989.
[3] L. Shen, L. Wu, Q. Sheng, C. Ma, Y. Zhang, L. Lu, J. Ma, J. Ma, J. Bian, Y. Yang, A. Chen, X. Lu, M. Liu, H. Wang, C. L. Jia, Advanced Materials, vol. 29, no. 33, pp. 1702411, 2017.
[4] M. Shahjahan, N. A. Ahmed, S. N. Rahman, S. Islam, N. Khatun, M. S. Hossain, International Journal of Innovative Technology and Exploring Engineering, vol. 3, no. 8, pp. 2278-3075, 2014.
[5] D. Bouokkeze, J. Massoudi, W. Hzez, M. Smari , A. Bougoffa, K. Khirouni, E. Dhahri, and L. Bessais, Royal Society of Chemistry RSC Adv., vol. 9, pp. 40940-40955, 2019.
[6] S. F. Mansour, F. Al-Hazmi, and M. A. Abdo, J. Alloys Compd. , vol.792, pp. 626–637, 2019.
[7] F.Xie, H. Liu, S. Zhou, Y. Chen, F. Xu, M. Bai, W. Liu, Journal of Alloys and Compounds**,** vol. 862, pp. 158650, 2021.
[8] S.A. Nikolaeva, E.N. Lysenko, E.V. Nikolaev, V.A. Vlasov, A.P. Surzhikov, Journal of Alloys and Compounds, vol. 941, pp. 169025, 2023.
[9] A.P. Surzhikov, A.V. Malyshev, E.N. Lysenko, V.A. Vlasov, A.N. Sokolovskiy, Ceramics International, vol. 43, pp. 9778-9782, 2017.
[10] A. V. Malyshev, E. N. Lysenko, A. V. Vlasov, S. A. Nikolaeva, Ceramics International, vol. 42, no. 4, pp. 16180-16183, 2016.
[11] C. Liu, Z. Lan, X. Jiang, Z. Yu, K. Sun, L. Li, P. Liu, Journal of Magnetism and Magnetic Materials, vol. 320, no. 7, pp. 1335-1339, 2008.
[12] K. L. Yadav, R. N. P. Chowdhary, Mater. Lett., vol. 19 pp. 61, 1994.
[13] A. B. Naik, J. I. Power, Ind. J. Pure Appl. Phys., vol. 23, pp. 436,1985.
[14] Rezlescu N., Condurach D., Petrariu P., Luca E., J. Am. Ceram. Soc., vol. 57, pp. 40, 1974.

[15] P. Kishan, D. R. Sagar, P. Swarup, J. Less Common Mater., vol.108, pp. 345, 1985.
[16] M. I. Klings, J. Phys. C8, pp. 3595, 1975.
[17] N. Rezlescu, D. Condurache, C. Naum, L. Luca, Rev. Roumaine Phys., vol. 18, pp. 727,1993.
[18] K. Muraleedharan, J. K. Srivastava, V. R. Marathe, R. Vijayaraghavan, J. A. Kulkarni, V. S. Darsane, Solid State Commun., vol. 55, pp. 363, 1985.
[19] N. Rezlescu, E. Rezlescu, ICF, vol.7, pp. 225,1997.
[20] B. Viswanathan, V. R. K. Murthy, Ferrite Materials Science and Technology, Narosa Publishing House, 1990.